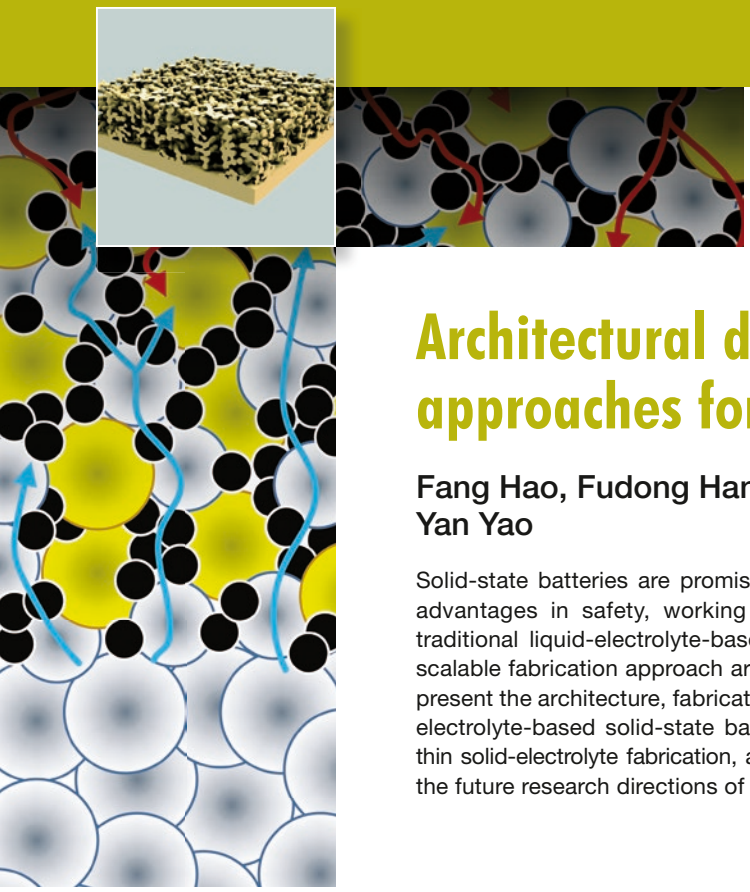


Architectural design and fabrication approaches for solid-state batteries

Fang Hao, Fudong Han, Yanliang Liang, Chunsheng Wang, and Yan Yao

Solid-state batteries are promising candidates for energy storage due to their potential advantages in safety, working temperature range, and energy density compared to traditional liquid-electrolyte-based batteries. Rational battery architecture design and a scalable fabrication approach are critical to realize solid-state batteries. In this article, we present the architecture, fabrication procedure, and related challenges of sulfide and oxide electrolyte-based solid-state batteries. Approaches toward intimate solid–solid contact, thin solid-electrolyte fabrication, and scale-up production are discussed. Finally, we discuss the future research directions of solid-state batteries.

Introduction

Solid-state batteries are receiving intense interest, especially because of the improved safety by replacing flammable liquid electrolytes with solid ones.[1] Solid-state batteries offer unique advantages over conventional liquid-electrolyte batteries including (1) the prevention of electrode cross-talk,[2] (2) the formation of a less dynamic interphase that does not continually reform during long-term cycling,[3] (3) the possibility for extremely high power and ultrathick electrode because of high concentration of metal ions per unit volume and the absence of an electrolyte concentration gradient,[4,5] and (4) the possibility for bipolar design wherein the negative plate of one cell is also the positive plate of the next cell.[6]

Despite these great promises, many challenges remain in both fundamental understanding and manufacturing of solid-state batteries. Although the ionic conductivities of solid electrolytes have approached those of liquid electrolytes,[7,8] a highly conductive solid electrolyte alone is still insufficient for a high-performance solid-state battery. The interfacial stability,[9–11] lithium dendrite suppression,[12–14] processing, and fabrication[6,15] are also critical for practical applications of solid-state batteries. In particular, market adoption of solid-state batteries requires large-scale fabrication at costs comparable to those for conventional lithium-ion batteries (LIBs), which has so far not been achieved. Here, we present our perspectives on the architectural design and fabrication approaches of solid-state batteries with the aim to promote their practical application.

Current architectures and fabrication approaches of solid-state batteries

Conventional LIBs use porous electrodes (both cathode and anode) and a porous separator with the pores filled with a liquid electrolyte.[16] On the other hand, solid-state batteries are usually made of dense layers of electrodes and electrolytes (**Figure 1**a). The use of dense layers is not only beneficial for high volumetric energy density, but also a prerequisite for intimate interfacial contact and fast Li^+ conduction. The cathode of solid-state batteries is usually a composite layer of an active material, an ionically conductive solid electrolyte, and electronically conductive carbon. Conductive carbon is excluded sometimes if the electronic conductivity of the active material is sufficiently high.[17–19] A high mechanical strength for the dense cathodes is required to sustain any volume change of the active materials since there is no free space to accommodate such changes. A dense layer of

Fang Hao, Department of Electrical and Computer Engineering, University of Houston, USA; fhao2@uh.edu
Fudong Han, Department of Chemical and Biomolecular Engineering, University of Maryland, USA; fdhan@umd.edu
Yanliang Liang, Department of Electrical and Computer Engineering, University of Houston, USA; yliang7@central.uh.edu
Chunsheng Wang, Department of Chemical and Biomolecular Engineering, University of Maryland, USA; cswang@umd.edu
Yan Yao, Department of Electrical and Computer Engineering and Texas Center for Superconductivity, University of Houston, USA; yyao4@uh.edu
doi:10.1557/mrs.2018.211

© 2018 Materials Research Society

https://doi.org/10.1557/mrs.2018.211 Published online by Cambridge University Press

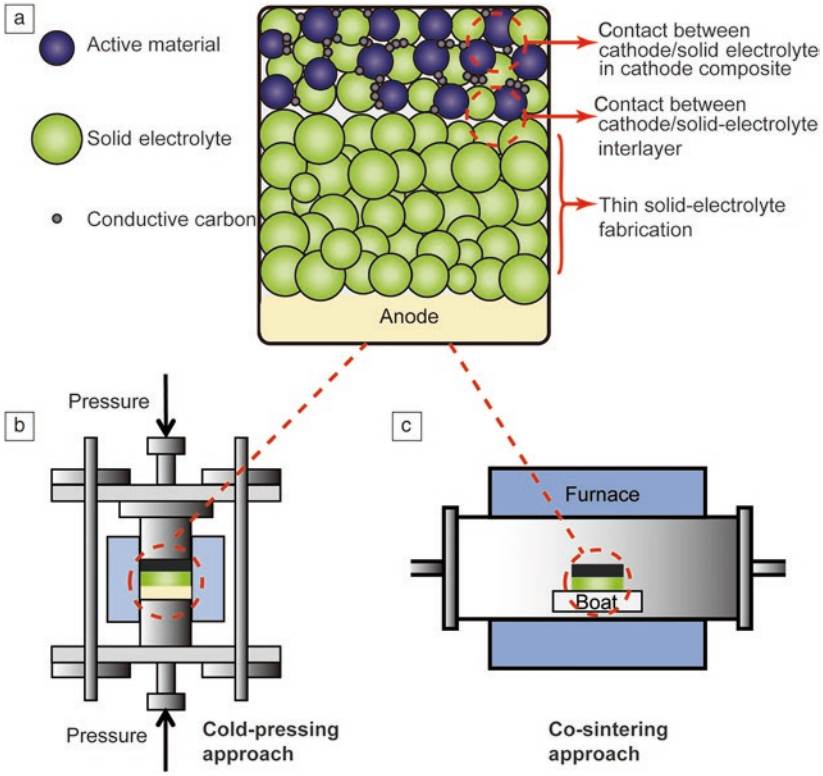


Figure 1. Schematics of the architecture and fabrication approaches for solid-state batteries. (a) Schematic representation of a typical bulk-type solid-state battery. (b) Cold-pressing process for sulfide solid electrolyte-based solid-state battery. (c) Sintering process for oxide solid electrolyte-based solid-state battery.

the solid electrolyte is also required to separate the cathode from the anode, which is also considered a potential solution for Li dendrite suppression and enabling high-capacity Li anodes.[20,21] However, challenges remain in understanding the formation of Li dendrites along the grain boundaries and voids in certain solid electrolytes.[12–14,22] If conventional anode materials such as graphite and $Li_4Ti_5O_{12}$ are used in solid-state batteries instead of Li metal, a composite electrode could also be used as the anode.

The fabrication approach for solid-state batteries largely depends on the mechanical properties of the solid electrolyte being used. Sulfide electrolytes are compliant, and therefore both the composite electrode and the solid electrolyte layer can be prepared by cold-pressing (Figure 1b),[23] and a lithium disc can be attached to the electrolyte with minimal pressure. However, oxide-based solid electrolytes generally have better mechanical strength,[24] and high-temperature sintering (Figure 1c) is usually required to ensure good contact within the solid electrolyte and at the interface between the solid electrolyte and the electrode.

Current approaches for preparing solid-state batteries cannot be easily scaled up to industrial production, and the performance of most solid-state batteries is not as good as those of liquid-electrolyte batteries. Figure 1a summarizes the main challenges for achieving a high-performance solid-state battery, including achieving intimate interfacial contact between the electrolyte and active material particles in the cathode composite, achieving intimate interfacial contact between the cathode composite layer and electrolyte layer, and fabricating a thin electrolyte layer. In addition, the bottleneck of scaling up for industrial fabrication is also discussed.

Intimate contact between active material and solid-electrolyte particles in cathode composite

An ionically and electronically conductive network in the cathode composite is crucial for high-performance solid-state batteries. Unlike conventional batteries where liquid electrolytes easily infiltrate into a porous cathode layer to form an intimate liquid–solid contact, solid-state batteries face challenges arising from insufficient solid–solid contact, leading to large interfacial resistance between the active material and solid-electrolyte particles.

Various approaches have been reported to increase the interparticle contact area in the cathode composite. A straightforward approach is to use submicrometer particles by mechanical milling of the active material, conductive carbon, and solid electrolyte using a planetary ball-mill apparatus.[25,26] Different from hand-ground cathode composite (**Figure 2**a), better contact was obtained with submicrometer particles, forming an effective ion- and electron-transport pathway (Figure 2b).[27] Further enhancement of the contact area can be achieved by using solution-processible components. Some of the prevailing options are soluble sulfide solid electrolytes.[28] A solution of the sulfides is either mixed with an active material to form solid electrolyte-coated active material after removing the solvent,[29–31] or infiltrated into a porous cathode fabricated for conventional liquid-electrolyte LIBs.[32] Both approaches allow active materials and solid electrolytes to form an intimate contact, and thus a more efficient ion-transport pathway as well as enhanced performance compared to dry-mixed electrodes.

In addition to ionic conduction, an electronic pathway should also be simultaneously improved. Therefore, a solution-processible conductive carbon precursor was proposed, where soluble poly(vinylpyrrolidone) was coprecipitated with an active material and a solid electrolyte followed by thermal carbonization (Figure 2c).[33] The mixed ionic and electronic conducting cathode composite shows intimate triple-phase contact in the nanoscale (Figure 2d), resulting in a high utilization of the active materials. For solid-oxide electrolytes with a low solubility in solvents, auxiliary liquid or solid wetting agents may be introduced to facilitate interfacial contact.

https://doi.org/10.1557/mrs.2018.211 Published online by Cambridge University Press

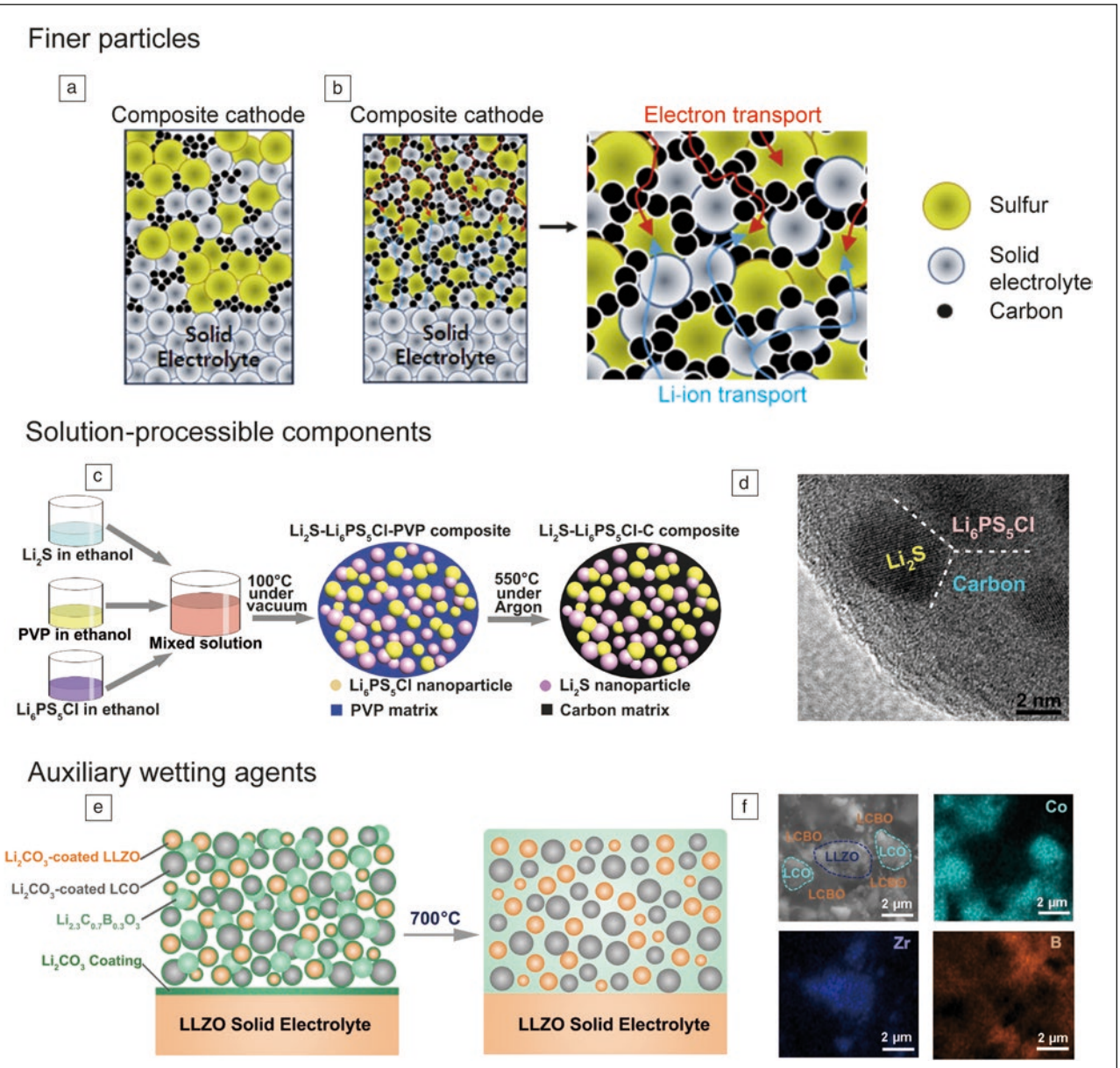


Figure 2. Schematics of approaches to improve contact between the active material and solid electrolyte particles in a cathode composite. (a) Cathode composite with large particles and limited contact area. (b) Cathode composite with finer particles and larger contact area. Reprinted with permission from Reference 27. © 2015 Elsevier. (c) Schematics of fabrication approach of mixed conducting cathode composite using solution-processible components. Reprinted with permission from Reference 33. © 2016 American Chemical Society. (d) Transmission electron microscope characterization of as-synthesized cathode composite. (e) Schematic of the cathode–electrolyte interface before and after co-sintering with an auxiliary wetting agent. (f) Cross-sectional scanning electron microscope image and elemental mapping images of cathode composite after sintering. Reprinted with permission from Reference 18. © 2018 Elsevier. Note: LCBO, $Li_{2.3-x}C_{0.7+x}B_{0.3-x}O_3$; LLZO, $Li_7La_3Zr_2O_{12}$; PVP, poly(vinylpyrrolidone).

Liquid electrolytes are great examples of such wetting agents, though the introduction of liquids compromises the unique properties of solid-state batteries.[34] Li_3BO_3 (LBO) is a solid wetting agent that has a melting point of 700°C, enabling improved interfacial contact between $Li_7La_3Zr_2O_{12}$ (LLZO) particles at a relatively low sintering temperature (790°C).[35] The introduced LBO can also minimize element mutual diffusion between the active material and the solid electrolytes, which takes place at >500°C by physically separating the two during sintering.[36] To further improve the contact and separation, the wetting agent $Li_{2.3}C_{0.7}B_{0.3}O_3$ reacts with Li_2CO_3 and forms a solid-solution interphase of $Li_{2.3-x}C_{0.7+x}B_{0.3-x}O_3$ (LCBO) after sintering at 700°C (Figure 2e). The active material and solid-electrolyte particles are tightly glued together by the presence of LCBO (Figure 2f).[18] Overall, an intimate interparticle contact is nontrivial to the formation of an ionically/electronically conductive network in a cathode composite and continues to call for more effective solutions.

https://doi.org/10.1557/mrs.2018.211 Published online by Cambridge University Press

Intimate contact between the cathode layer and solid-electrolyte layer

In addition to the contact within the cathode composite, contact between the cathode layer and electrolyte layer can also become problematic. Due to the excellent deformability of sulfide solid electrolytes, intimate contact is achieved by simple cold-pressing. However, a rigid oxide solid electrolyte can leave microscopic gaps between the cathode and the solid-electrolyte layers and cause huge interfacial resistance (**Figure 3**a). The interfacial contact can be improved by the previously mentioned wetting agent-aided co-sintering,[35] or by advanced sintering techniques such as spark plasma sintering that could lower the sintering temperature (680°C) and shorten processing time (10 min).[37] However, element mutual diffusion inevitably occurs at these temperatures (>500°C) and induces resistive interphase formation.

Insertion of auxiliary interlayers has been proposed to improve the interlayer contact without degrading interface stability. A thin Nb layer was deposited on the surface of a LLZO pellet by radio-frequency magnetron sputtering and thermal annealing to form an Li^+-conductive Li-Nb-O layer (Figure 3b). The interfacial resistance between $LiCoO_2$ and LLZO decreased from 2600 Ω cm^2 to 150 Ω cm^2 after the introduction of the Li-Nb-O interlayer, which was attributed to the elimination of voids/cavities and the suppression of element diffusion at the interface.[38] Alternatively, an additional soft polymer electrolyte layer inserted between the cathode and solid-electrolyte layer (Figure 3c) can wet the oxide solid-electrolyte surface, leading to a large interlayer contact area.[39]

In addition to the interlayer approach, a monolithic porous cathode-dense electrolyte bilayer architecture represents a promising strategy to provide intimate contact and continuous ion transport if the active materials in the continuous porous channels can maintain good contact with the electrolyte wall during charge/discharge cycles.[40–43] The dense electrolyte layer was fabricated by tape casting an LLZO powder slurry while the porous electrolyte structure in cathodes was fabricated by adding a "pore former" (e.g., poly[methyl methacrylate]) in the slurry using the same method.

Finally, the monolithic bilayer structure was formed by laminating and co-sintering (Figure 3d).[43] The continuous connected pore channels in the porous layer allow subsequent infiltration of carbon nanotube ink and melted sulfur as the active materials. The direct connection between the cathode and solid electrolyte layers was demonstrated through elemental mapping (Figure 3e [La, red; S, green]). The previously discussed approaches can also be extended to improve the interfacial contact between anode and solid electrolyte.[44,45]

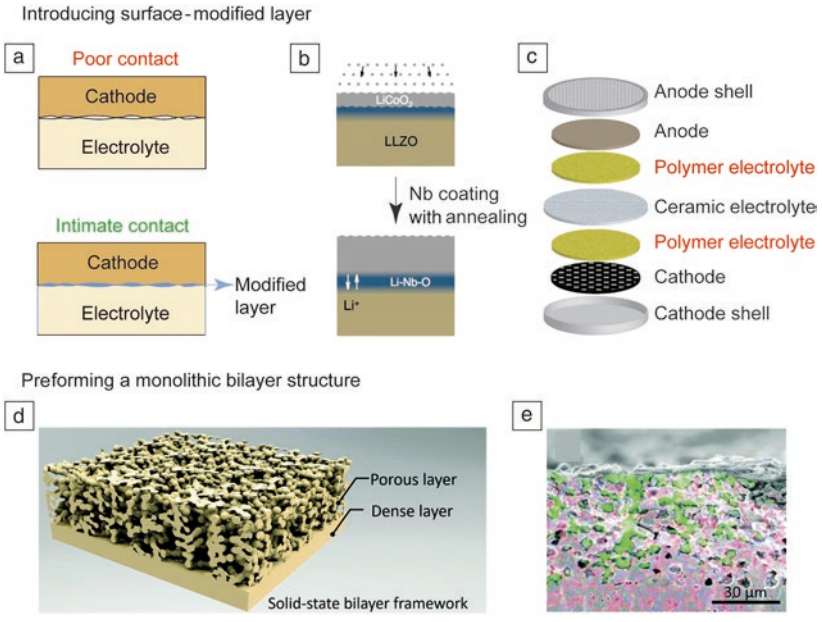


Figure 3. Schematics of approaches to improve the cathode-solid electrolyte interfacial contact. (a) Schematic representation of interlayer contact improvement by a surface modified layer. (b) Schematic representation of a Nb-modified interface, suppressing elemental diffusion and facilitating the contact area. Reprinted with permission from Reference 38. © 2014 Elsevier. (c) Schematic representation of solid-state battery design with a conductive polymer at the cathode–electrolyte interface. Reprinted with permission from Reference 39. © 2016 American Chemical Society. (d) Schematic representation of preformed monolithic bilayer structure after sintering. (e) Elemental mapping image (La in red; S in green) shows sulfur distribution and interconnectivity of bilayer framework. Reprinted with permission from Reference 43. © 2017 Royal Society of Chemistry.

Thin solid electrolyte fabrication

To achieve higher specific gravimetric energy (Wh kg^{-1}) and volumetric energy density (Wh L^{-1}) at the cell level than those of liquid-electrolyte LIBs, the solid electrolyte layer must be thinner than a critical value, or "break-even thickness."[46,47] For example, for a cathode with 19.5 mg cm^{-2} loading, the specific gravimetric energy break-even thickness for oxide (LLZO) and sulfide solid electrolyte layers ($Li_{10}GeP_2S_{12}$ [LGPS]) is 45 μm and 122 μm, respectively.[46] The sulfide-based solid electrolyte with a smaller mass density (LGPS, ρ ~ 2 g cm^{-3}; LLZO, ρ ~ 5 g cm^{-3}) shows a larger break-even thickness. Solid electrolytes with less than 120-μm thickness are necessary, which is still hard to reach using traditional fabrication. Thus, novel thin-electrolyte fabrication methods are essential.

Advanced techniques are emerging for fabricating thin oxide solid electrolytes with extremely conformal thin-coating quality such as pulsed laser deposition,[48] sol-gel,[49] aerosol deposition,[50] radio-frequency magnetron sputtering,[51] and atomic layer deposition,[52] though some of these approaches can be high cost and difficult to scale up. A scalable fabrication of a thin LLZO film was demonstrated with casting-sintering flame-made LLZO nanopowders.[53]

https://doi.org/10.1557/mrs.2018.211 Published online by Cambridge University Press

While typical LLZO pellets prepared from micropowders require sintering at >1000°C, the nanopowder-derived film was sintered at 700–800°C and was considerably dense and thin (<30 μm). Stacking such brittle thin films without damage is a challenge.

The break-even thickness for sulfide-solid electrolytes is larger than that for oxide-solid electrolytes, and thus technically easier to achieve.[46] Therefore, sulfide-solid electrolytes could be more promising for high cell-level specific energy and energy density.[54–59] Thin sulfide-solid electrolytes can be fabricated with the help of a compliant polymer scaffold.[55] **Figure 4**a shows a self-standing and bendable thin sulfide solid electrolyte layer (70 μm) fabricated by coating an Li_3PS_4 slurry on an Ni foil, followed by drying and cold-pressing onto a polymer (poly[para-phenylene terephthalamide]) nonwoven scaffold, which provides flexibility and toughness. The solid-state battery assembled using this thin solid electrolyte delivered a threefold increase in cell-level specific energy compared with that of a conventional pelletized solid-state battery.[55] Introducing polymeric binders also provides the mechanical flexibility and adhesion between solid electrolyte particles necessary for achieving a thin layer.[56,58] A thin solid electrolyte sheet (~70 μm) was prepared by coating a slurry consisting of glassy Li_3PS_4 solid electrolyte and styrene-butadiene-styrene copolymer binder on a copper foil.[56] Since polymer binders are ionic insulating, a thermal decomposable poly(propylene carbonate) binder was designed for fabricating thin glassy Li_3PS_4 sheets (~60 μm).[57] The binder could be fully removed by heat treatment at 225°C after stacking and compressing steps (Figure 4b). The solid-state battery thus formed exhibited cell-level specific energy of 115 Wh kg^{-1}, a 25% increase from that of the binder-containing solid-state battery (92 Wh kg^{-1}).[59]

Challenges for large-scale fabrication

Bringing solid-state batteries to the market requires scaling up from lab-scale fabrication to industrial production. In this section, we provide an overview of the main challenges for the large-scale fabrication of solid-state batteries.

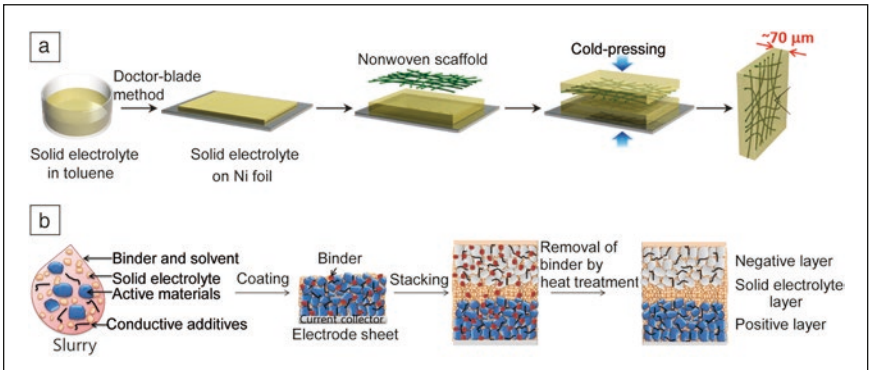


Figure 4. Fabrication approaches of solid-state batteries with thin solid electrolytes. (a) Schematic representation of fabrication of thin solid electrolyte with polymer scaffold. Reprinted with permission from Reference 55. © 2015 American Chemical Society. (b) Schematic representation of fabrication of binder-free styrene-butadiene-styrene. Reprinted with permission from Reference 57. © 2018 Nature Publishing Group.

Material cost

Solid-state batteries face challenges in obtaining low-cost solid electrolytes. The germanium in LGPS, one of the most promising solid electrolytes with an ionic conductivity of 12 mS cm^{-1} at room temperature, which surpasses those of liquid electrolytes, makes it expensive. Efforts are being made to find a substitution such as silicon or tin.[60] For oxide-solid electrolytes such as LLZO, lanthanum in garnet oxides is a concern because of its scarcity. Developing low-lanthanum oxide solid electrolytes could be a new direction. Similar to conventional LIBs, low-cost electrodes such as low-cobalt cathodes[61] and organic electrodes[62,63] are desirable for solid-state batteries.

Mass loading, layer thickness/density/uniformity

One unique advantage of solid-state batteries is that they can use thick electrodes because of the absence of an Li-ion concentration gradient and a high concentration of Li^+ ions per volume.[4] A 600-μm-thick cathode layer, corresponding to a geometric capacity of 15.7 mAh cm^{-2}, has been used in solid-state batteries with a sulfide-solid electrolyte.[5] Achieving homogenous distributions of solid electrolyte, active material, and carbon in such a thick electrode is challenging. It is found that the rate performance of an ultrathick electrode (600 μm) is mainly limited by the ohmic resistance from ion transport, and therefore more careful optimization is needed to improve the ionic conductivity of the solid electrolyte in the composite and lowering the tortuosity for Li^+ transport.[5] In this regard, a sintering step may be used for the cathode composite made of a sulfide solid electrolyte to improve the ionic conductivity of the cathode composite. Considerable attention must be focused on the particle size, morphology, and distribution of solid electrolyte particles to reduce the tortuosity. Although achieving close to theoretical density in the cathode composite is strongly desired, such a dense cathode composite may suffer severe mechanical strain/stress due to volume change of the electrode.[64] Adding polymer binders in the cathode composite can help tolerate the volumetric change of active materials and prevent the formation of stress-induced cracks.[65]

Fabrication environment

Sulfide electrolytes are sensitive to moisture in the air, generating toxic H_2S, and therefore the electrolytes and electrode composites have to be synthesized and processed in a moisture-controlled environment. Oxide electrolytes are more stable in air. However, reactions among LLZO, CO_2, and H_2O also occur, eventually forming Li_2CO_3 on the surface.[66] The formation of Li_2CO_3 on the surface affects the performance of LLZO (e.g., increased interfacial resistance between electrolyte and Li).[67] Several approaches have been proposed to remove the Li_2CO_3 layer on LLZO.[68,69]

https://doi.org/10.1557/mrs.2018.211 Published online by Cambridge University Press

All of these approaches should be carried out in an inert atmosphere to avoid the reformation of Li_2CO_3 during processing. In addition, the environment for sintering of oxide-based electrolytes is important. Subtle variations in humidity, Li vapor pressure, and CO_2 and O_2 partial pressures have a strong influence on the relative density and ionic conductivity of a solid electrolyte.[15] Sintering under an O_2 atmosphere helps to achieve a high relative density and ionic conductivity for LLZO.[70]

Cell stacking

Although the utilization of solid electrolytes enables bipolar design, stacking solid-state batteries for a high-voltage cell pack has been difficult. Currently, the stacking of multiple cells is achieved manually.[71] The key challenge arises from the high bending stiffness of electrode and electrolyte layers. It should be ensured that the layers remain undamaged during stacking. Pressure or heating may be needed to ensure intimate contact between layers. In addition, the volume change of a stacked cell during charge and discharge is another issue to be addressed. Polymer binders may be added in each layer and buffer space may be required to accommodate the volume change.[72] Fixed or variable pressure can be applied on the cell stack during cycling. Packaging will also require a special design to address the volume change.

Summary and outlook

We have reviewed architectures of solid-state batteries and highlighted fabrication approaches for achieving intimate interparticle and interlayer contact. The contact evolution upon cycling, however, is not well understood, and alternative materials, cathode configurations, and fabrication approaches may be needed to maintain excellent interfacial contact during battery cycling. The thin solid electrolyte film is critical for high cell-level specific energy and energy density. Thin solid electrolyte films are prepared from soluble solid electrolytes with the aid of polymer scaffolds or binders. However, not all solid electrolytes are soluble, and ionic insulating polymer scaffolds or binders can compromise ion conduction. Soluble solid electrolytes with high ionic conductivity and polymer binders removable at low temperatures are therefore highly desirable. For integration of thin solid-electrolyte films into solid-state batteries, a cathode-supported solid-state battery, similar to a cathode-supported solid oxide fuel cell,[73] may be developed. Future research for solid-state battery fabrication will be directed toward large-scale approaches; roll-to-roll fabrication and three-dimensional printing are worth considering in this regard.

Acknowledgments

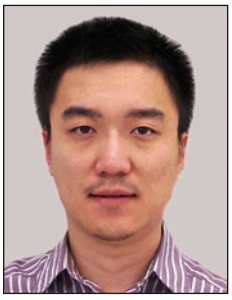
Y.Y., F.H., and Y.L. acknowledge funding support from the US Department of Energy's Office of Energy Efficiency and Renewable Energy (EERE), as part of the Battery 500 Consortium (Award No. DE-EE0008234). C.W. and F.H. gratefully acknowledge the support of the Army Research Office under Award No. W911NF1510187.

References

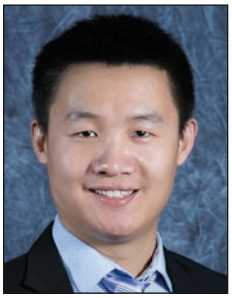
1. J. Janek, W.G. Zeier, *Nat. Energy* **1**, 16141 (2016).
2. Y.V. Mikhaylik, J.R. Akridge, *J. Electrochem. Soc.* **151**, A1969 (2004).
3. A.C. Luntz, J. Voss, K. Reuter, *J. Phys. Chem. Lett.* **6**, 4599 (2015).
4. Y. Kato, S. Hori, T. Saito, K. Suzuki, M. Hirayama, A. Mitsui, M. Yonemura, H. Iba, R. Kanno, *Nat. Energy* **1**, 16030 (2016).
5. Y. Kato, S. Shiotani, K. Morita, K. Suzuki, M. Hirayama, R. Kanno, *J. Phys. Chem. Lett.* **9**, 607 (2018).
6. J. Schnell, T. Günther, T. Knoche, C. Vieider, L. Köhler, A. Just, M. Keller, S. Passerini, G. Reinhart, *J. Power Sources* **382**, 160 (2018).
7. J.C. Bachman, S. Muy, A. Grimaud, H.-H. Chang, N. Pour, S.F. Lux, O. Paschos, F. Maglia, S. Lupart, P. Lamp, L. Giordano, Y. Shao-Horn, *Chem. Rev.* **116**, 140 (2016).
8. V. Thangadurai, S. Narayanan, D. Pinzaru, *Chem. Soc. Rev.* **43**, 4714 (2014).
9. F. Han, Y. Zhu, X. He, Y. Mo, C. Wang, *Adv. Energy Mater.* **6**, 1501590 (2016).
10. R. Koerver, I. Aygün, T. Leichtweiß, C. Dietrich, W. Zhang, J.O. Binder, P. Hartmann, W.G. Zeier, J. Janek, *Chem. Mater.* **29**, 5574 (2017).
11. F. Han, T. Gao, Y. Zhu, K.J. Gaskell, C. Wang, *Adv. Mater.* **27**, 3473 (2015).
12. Y. Ren, Y. Shen, Y. Lin, C.-W. Nan, *Electrochem. Commun.* **57**, 27 (2015).
13. E.J. Cheng, A. Sharafi, J. Sakamoto, *Electrochim. Acta* **223**, 85 (2017).
14. F. Han, J. Yue, X. Zhu, C. Wang, *Adv. Energy Mater.* **8**, 1703644 (2018).
15. K. Kerman, A. Luntz, V. Viswanathan, Y.-M. Chiang, Z. Chen, *J. Electrochem. Soc.* **164**, A1731 (2017).
16. T. Knoche, V. Zinth, M. Schulz, J. Schnell, R. Gilles, G. Reinhart, *J. Power Sources* **331**, 267 (2016).
17. N. Kamaya, K. Homma, Y. Yamakawa, M. Hirayama, R. Kanno, M. Yonemura, T. Kamiyama, Y. Kato, S. Hama, K. Kawamoto, A. Mitsui, *Nat. Mater.* **10**, 682 (2011).
18. F. Han, J. Yue, C. Chen, N. Zhao, X. Fan, Z. Ma, T. Gao, F. Wang, X. Guo, C. Wang, *Joule* **2**, 497 (2018).
19. W. Zhang, T. Leichtweiß, S.P. Culver, R. Koerver, D. Das, D.A. Weber, W.G. Zeier, J. Janek, *ACS Appl. Mater. Interfaces* **9**, 35888 (2017).
20. C. Monroe, J. Newman, *J. Electrochem. Soc.* **152**, A396 (2005).
21. B.J. Neudecker, N.J. Dudney, J.B. Bates, *J. Electrochem. Soc.* **147**, 517 (2000).
22. L. Porz, T. Swamy, B.W. Sheldon, D. Rettenwander, T. Frömling, H.L. Thaman, S. Berendts, R. Uecker, W.C. Carter, Y.-M. Chiang, *Adv. Energy Mater.* **7**, 1701003 (2017).
23. A. Sakuda, A. Hayashi, M. Tatsumisago, *Sci. Rep.* **3**, 2261 (2013).
24. S. Yu, R.D. Schmidt, R. Garcia-Mendez, E. Herbert, N.J. Dudney, J.B. Wolfenstine, J. Sakamoto, D.J. Siegel, *Chem. Mater.* **28**, 197 (2016).
25. M. Nagao, A. Hayashi, M. Tatsumisago, *Electrochim. Acta* **56**, 6055 (2011).
26. M. Nagao, A. Hayashi, M. Tatsumisago, *J. Mater. Chem.* **22**, 10015 (2012).
27. H.U. Choi, J.S. Jin, J.-Y. Park, H.-T. Lim, *J. Alloys Compd.* **723**, 787 (2017).
28. Z. Liu, W. Fu, E.A. Payzant, X. Yu, Z. Wu, N.J. Dudney, J. Kiggans, K. Hong, A.J. Rondinone, C. Liang, *J. Am. Chem. Soc.* **135**, 975 (2013).
29. Z. Lin, Z. Liu, N.J. Dudney, C. Liang, *ACS Nano* **7**, 2829 (2013).
30. S. Teragawa, K. Aso, K. Tadanaga, A. Hayashi, M. Tatsumisago, *J. Mater. Chem. A* **2**, 5095 (2014).
31. Y.E. Choi, K.H. Park, D.H. Kim, D.Y. Oh, H.R. Kwak, Y.-G. Lee, Y.S. Jung, *ChemSusChem* **10**, 2605 (2017).
32. D.H. Kim, D.Y. Oh, K.H. Park, Y.E. Choi, Y.J. Nam, H.A. Lee, S.-M. Lee, Y.S. Jung, *Nano Lett.* **17**, 3013 (2017).
33. F. Han, J. Yue, X. Fan, T. Gao, C. Luo, Z. Ma, L. Suo, C. Wang, *Nano Lett.* **16**, 4521 (2016).
34. H. Huo, N. Zhao, J. Sun, F. Du, Y. Li, X. Guo, *J. Power Sources* **372**, 1 (2017).
35. S. Ohta, J. Seki, Y. Yagi, Y. Kihira, T. Tani, T. Asaoka, *J. Power Sources* **265**, 40 (2014).
36. K. Park, B.-C. Yu, J.-W. Jung, Y. Li, W. Zhou, H. Gao, S. Son, J.B. Goodenough, *Chem. Mater.* **28**, 8051 (2016).
37. A. Aboulaich, R. Bouchet, G. Delaizir, V. Seznec, L. Tortet, M. Morcrette, P. Rozier, J.-M. Tarascon, V. Viallet, M. Dollé, *Adv. Energy Mater.* **1**, 179 (2011).
38. T. Kato, T. Hamanaka, K. Yamamoto, T. Hirayama, F. Sagane, M. Motoyama, Y. Iriyama, *J. Power Sources* **260**, 292 (2014).
39. W. Zhou, S. Wang, Y. Li, S. Xin, A. Manthiram, J.B. Goodenough, *J. Am. Chem. Soc.* **138**, 9385 (2016).
40. Y. Ren, T. Liu, Y. Shen, Y. Lin, C.-W. Nan, *Ionics* **23**, 2521 (2017).
41. J. van den Broek, S. Afyon, J.L.M. Rupp, *Adv. Energy Mater.* **6**, 1600736 (2016).
42. Y. Gong, K. Fu, S. Xu, J. Dai, T.R. Hamann, L. Zhang, G.T. Hitz, Z. Fu, Z. Ma, D.W. McOwen, X. Han, L. Hu, E.D. Wachsman, *Mater. Today* **21**, 594 (2018).
43. K. Fu, Y. Gong, G.T. Hitz, D.W. McOwen, Y. Li, S. Xu, Y. Wen, L. Zhang, C. Wang, G. Pastel, J. Dai, B. Liu, H. Xie, Y. Yao, E.D. Wachsman, L. Hu, *Energy Environ. Sci.* **10**, 1568 (2017).
44. X. Han, Y. Gong, K. Fu, X. He, G.T. Hitz, J. Dai, A. Pearse, B. Liu, H. Wang, G. Rubloff, Y. Mo, V. Thangadurai, E.D. Wachsman, L. Hu, *Nat. Mater.* **16**, 572 (2016).

https://doi.org/10.1557/mrs.2018.211 Published online by Cambridge University Press

45. C. Yang, L. Zhang, B. Liu, S. Xu, T. Hamann, D. McOwen, J. Dai, W. Luo, Y. Gong, E.D. Wachsman, L. Hu, *Proc. Natl. Acad. Sci. U.S.A.* **115**, 3770 (2018).
46. B. Wu, S. Wang, W.J. Evans IV, D.Z. Deng, J. Yang, J. Xiao, *J. Mater. Chem. A* **4**, 15266 (2016).
47. B.D. McCloskey, *J. Phys. Chem. Lett.* **6**, 4581 (2015).
48. S. Kim, M. Hirayama, S. Taminato, R. Kanno, *Dalton Trans.* **42**, 13112 (2013).
49. R.-J. Chen, M. Huang, W.-Z. Huang, Y. Shen, Y.-H. Lin, C.-W. Nan, *J. Mater. Chem. A* **2**, 13277 (2014).
50. C.-W. Ahn, J.-J. Choi, J. Ryu, B.-D. Hahn, J.-W. Kim, W.-H. Yoon, J.-H. Choi, D.-S. Park, *J. Electrochem. Soc.* **162**, A60 (2015).
51. S. Lobe, C. Dellen, M. Finsterbusch, H.G. Gehrke, D. Sebold, C.L. Tsai, S. Uhlenbruck, O. Guillon, *J. Power Sources* **307**, 684 (2016).
52. E. Kazyak, K.-H. Chen, K.N. Wood, A.L. Davis, T. Thompson, A.R. Bielinski, A.J. Sanchez, X. Wang, C. Wang, J. Sakamoto, N.P. Dasgupta, *Chem. Mater.* **29**, 3785 (2017).
53. E. Yi, W. Wang, J. Kieffer, R.M. Laine, *J. Mater. Chem. A* **4**, 12947 (2016).
54. T. Inada, T. Kobayashi, N. Sonoyama, A. Yamada, S. Kondo, M. Nagao, R. Kanno, *J. Power Sources* **194**, 1085 (2009).
55. Y.J. Nam, S.-J. Cho, D.Y. Oh, J.-M. Lim, S.Y. Kim, J.H. Song, Y.-G. Lee, S.-Y. Lee, Y.S. Jung, *Nano Lett.* **15**, 3317 (2015).
56. A. Sakuda, K. Kuratani, M. Yamamoto, M. Takahashi, T. Takeuchi, H. Kobayashi, *J. Electrochem. Soc.* **164**, A2474 (2017).
57. M. Yamamoto, Y. Terauchi, A. Sakuda, M. Takahashi, *Sci. Rep.* **8**, 1212 (2018).
58. K. Lee, S. Kim, J. Park, S.H. Park, A. Coskun, D.S. Jung, W. Cho, J.W. Choi, *J. Electrochem. Soc.* **164**, A2075 (2017).
59. D.Y. Oh, D.H. Kim, S.H. Jung, J.-G. Han, N.-S. Choi, Y.S. Jung, *J. Mater. Chem. A* **5**, 20771 (2017).
60. S.P. Ong, Y. Mo, W.D. Richards, L. Miara, H.S. Lee, G. Ceder, *Energy Environ. Sci.* **6**, 148 (2013).
61. E.A. Olivetti, G. Ceder, G.G. Gaustad, X. Fu, *Joule* **1**, 229 (2017).
62. Y. Liang, Y. Jing, S. Gheytani, K.-Y. Lee, P. Liu, A. Facchetti, Y. Yao, *Nat. Mater.* **16**, 841 (2017).
63. X. Chi, Y. Liang, F. Hao, Y. Zhang, J. Whiteley, H. Dong, P. Hu, S. Lee, Y. Yao, *Angew. Chem. Int. Ed. Engl.* **57**, 2630 (2018).
64. G. Bucci, T. Swamy, Y.-M. Chiang, W.C. Carter, *J. Mater. Chem. A* **5**, 19422 (2017).
65. R.-J. Chen, Y.-B. Zhang, T. Liu, B.-Q. Xu, Y.-H. Lin, C.-W. Nan, Y. Shen, *ACS Appl. Mater. Interfaces* **9**, 9654 (2017).
66. Y. Wang, W. Lai, *J. Power Sources* **275**, 612 (2015).
67. L. Cheng, E.J. Crumlin, W. Chen, R. Qiao, H. Hou, S.F. Lux, V. Zorba, R. Russo, R. Kostecki, Z. Liu, K. Persson, W. Yang, J. Cabana, T. Richardson, G. Chen, M. Doeff, *Phys. Chem. Chem. Phys.* **16**, 18294 (2014).
68. A. Sharafi, E. Kazyak, A.L. Davis, S. Yu, T. Thompson, D.J. Siegel, N.P. Dasgupta, J. Sakamoto, *Chem. Mater.* **29**, 7961 (2017).
69. Y. Li, X. Chen, A. Dolocan, Z. Cui, S. Xin, L. Xue, H. Xu, K. Park, J.B. Goodenough, *J. Am. Chem. Soc.* **140**, 6448 (2018).
70. Y. Li, Z. Wang, C. Li, Y. Cao, X. Guo, *J. Power Sources* **248**, 642 (2014).
71. S. Ito, S. Fujiki, T. Yamada, Y. Aihara, Y. Park, T.Y. Kim, S.-W. Baek, J.-M. Lee, S. Doo, N. Machida, *J. Power Sources* **248**, 943 (2014).
72. T. Inada, K. Takada, A. Kajiyama, H. Sasaki, S. Kondo, M. Watanabe, M. Murayama, R. Kanno, *J. Power Sources* **119–121**, 948 (2003).
73. N.H. Menzler, F. Tietz, S. Uhlenbruck, H.P. Buchkremer, D. Stöver, *J. Mater. Sci.* **45**, 3109 (2010). □



Fang Hao is a doctoral candidate in the Department of Electrical and Computer Engineering at the University of Houston. He received his BS degree from the University of Electronic Science and Technology of China in 2011 and his MS degree from Boston University in 2013. His research mainly focuses on materials and device architectures for all-solid-state batteries. Hao can be reached by email at fhao2@uh.edu.



Fudong Han is a postdoctoral associate at the University of Maryland. He received his BS degree in 2009 and his MS degree in 2012 in Materials Science and Engineering from Shandong University, China, and his PhD degree in Chemical and Biomolecular Engineering from the University of Maryland, College Park, in 2018. His research focuses on all-solid-state batteries. He is the recipient of a 2017 MRS Graduate Student Gold Award and 2018 ECS Battery Division Student Research Award. Han can be reached by email at fdhan@umd.edu.



Yanliang Liang is a research associate in the Department of Electrical and Computer Engineering at the University of Houston. He received his PhD degree from Nankai University, China, in 2012. His main research interests concern material design, system development, and mechanistic understanding for battery technologies. He has published 37 papers and 10 patents in the field of energy storage and conversion. Liang can be reached by email at yliang7@central.uh.edu.



Chunsheng Wang is a professor in the Department of Chemical and Biomolecular Engineering and the Department of Chemistry and Biochemistry at the University of Maryland (UMD). He is an associate editor of the journal *ACS Applied Energy Materials*, and UMD director of the Center for Research in Extreme Batteries, a joint battery center between the US Army Research Laboratory and the University of Maryland. He received his PhD degree in materials science and engineering from Zhejiang University, China, in 1995. Prior to joining UMD in 2007, he was an assistant professor in the Department of Chemical Engineering at Tennessee Technological University (2003–2007) and a research scientist in the Center for Electrochemical System and Hydrogen Research at Texas A&M University (1998–2003). His research focuses on rechargeable batteries and fuel cells. Wang can be reached by email at cswang@umd.edu.



Yan Yao is an associate professor in the Department of Electrical and Computer Engineering at the University of Houston and Texas Center for Superconductivity (TcSUH). He received his PhD degree in materials science and engineering from the University of California, Los Angeles, in 2008. Prior to joining the University of Houston as an assistant professor in 2012, he was a senior scientist at Polyera Corporation (now Flexterra) from 2008 to 2010 and a postdoctoral fellow at Stanford University from 2010 to 2012. His current research interests include magnesium batteries, aqueous batteries, solid-state batteries, and organic battery materials. Yao can be reached by email at yyao4@uh.edu.



https://doi.org/10.1557/mrs.2018.211 Published online by Cambridge University Press